STATISTICAL MECHANICAL ANALYSIS OF RAMAN SPECTROSCOPIC ORDER PARAMETER CHANGES IN PRESSURE-INDUCED LIPID BILAYER PHASE TRANSITIONS

PAUL YAGER AND WARNER L. PETICOLAS, *Department of Chemistry, University of Oregon, Eugene, Oregon 97403 U.S.A.*

ABSTRACT The statistical mechanical cluster theory of Fisher as applied by Kanehisa and Tsong to phopholipid bilayers is modified to describe the effects of hydrostatic pressure on the state of an aqueous dispersion of the phospholipid dipalmitoyl phosphatidylcholine. A high pressure Raman scattering cell has been built to obtain the Raman spectra of aqueous dispersions of phospholipids as a function of the applied hydrostatic pressure from 0 to 100 atmospheres. Predicted thermal and pressure-induced phase transitions are compared with an experimentally obtained Raman order parameter derived from the ratio of two bands in the C-H stretching region of the Raman spectrum of the sample. The parameters of the theory are adjusted to obtain a satisfactory fit of the Raman order parameter versus temperature. The theory is then found to give an excellent prediction of the observed pressure dependence of the Raman order parameter with no changes in the adjustable parameters. The implications of the success of the theoretical fit is discussed. Particularly of interest is the rather high value of the critical temperature, Tc, for lipid bilayers which is predicted by the model.

INTRODUCTION

The physical chemical properties of biological membranes or lipid bilayers have been studied by many techniques, and many of the basic properties of both the complex natural membranes and various model systems are now known (1–4). Work in our laboratory has explored the nature of phase changes in the very simple and widely studied model system of dipalmitoyl phosphatidylcholine by Raman scattering techniques (5–8). Thus we are particularly interested in using a Raman spectroscopic determination of membrane order to test theoretical models which have been applied to this system. We have begun with the Fisher cluster model used by Kanehisa and Tsong (9) to explain the thermodynamic behavior of this system. We have extended the theory to the description of phase transitions induced by changes in hydrostatic pressure.

A number of workers have studied both the change in volume upon melting (10, 11), and the change in the melting point, T_m, upon increases in pressure (12–14) of this and other phospholipid dispersion systems. With knowledge of the ΔV of transition for the system and the work of Kanehisa and Tsong on temperature induced transitions, we set out to modify the theory to apply it to our data on the pressure-induced transitions. With the extended cluster theory it is possible to predict the order as a function of both temperature, T, and pressure, P.

MATERIALS AND METHODS

The L isomer of dipalmitoyl phosphatidylcholine (DPPC) was purchased from Sigma Chemical Co., St. Louis, Mo., and purified by column chromatography on Sephadex LH-20 in 95% ethanol. Dispersions were prepared by gentle agitation of dry purified DPPC coated on a round-bottomed flask with distilled H_2O at temperatures near and above T_m. The sample so prepared was injected with a syringe into the high pressure Raman cell and centrifuged at low speed until the injected volume completely separated into a turbid pellet and a clear supernate. All Raman measurements were performed on the pellet. Variable pressures were generated by a high-pressure regulator (Victor Comptometer Corp., Chicago, Ill.) used to step down the pressure in a tank of helium. ~0.5 m of distilled H_2O separated the sample from the helium to minimize dissolution of He in the sample.

The high pressure Raman cell, shown in Fig. 1, is built around a fused quartz tube with an o.d. of 7 mm and an i.d. of 0.5 mm. One end is melted closed and the other is carefully flared, keeping the i.d. fairly constant. The flared end is held in place in a brass cup with a seal of epoxy highly filled with silica. The flared end of the quartz tube is fixed sufficiently below the end of the brass cup to ensure that the mechanical stress produced by sealing the cell is not directly applied to the brittle quartz. If not exposed to great extremes of temperature (i.e., kept between 0° and 70°C), not mechanically or thermally shocked, the brass-to-epoxy-to-quartz seal will not leak water to pressures of 2,000 psi. This unit, the cell, can be centrifuged at low speeds if an appropriate holder (supporting the cell by the brass cup) is fashioned, and at least one carefully balanced matching set is constructed.

Sealing the cell to the high pressure system is accomplished by pressing a brass plug of matching diameter against the cup with an interposing neoprene o-ring. Certain factors are important for safety and efficiency: (*a*) The cells may explode because imperceptible flaws in the quartz may grow under pressure causing the shaft of the tube and brass cap to separate. Consequently the rod must be encased in an adequate brass shield. A heavy brass blast shield design proved adequate on several occasions. (*b*) To prevent the projectile from exiting the blast shield and attaining a high velocity in case of fracture near the epoxy seal (the most common break point) and to facilitate removal of the cell from the holder it is convenient to thread the end of the hole near the tip of the tube and place a hand-turnable bolt in it. This bolt should fit almost to the end of the quartz tube, but not touch it. (*c*) There must be observation holes to view the capillary and allow both entrance and exit of the laser beam. For safety these should be of the minimum practical size. (*d*) For temperature control, hollow copper tubing can easily be soft-soldered to the block. However, a series of narrow tubes in parallel is preferable to one long narrow tube when used with a circulating water bath due to the high resistance to flow of such tubing.

In our system the entire cell is held in place and kept thermally isolated from the sample support stage by a Lucite mounting block. When used with a Lauda refrigerated circulating water bath (Lauda Div.,

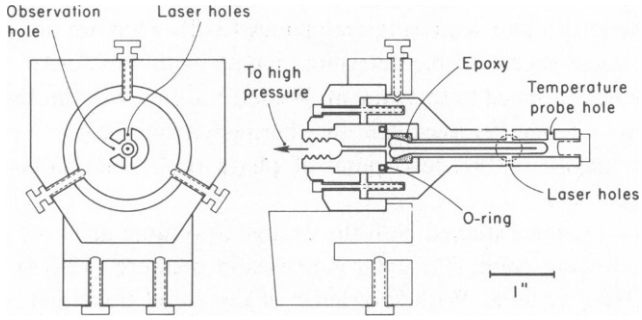

FIGURE 1 The high-pressure Raman cell, mounted in its Lucite holder and shown from the front and side in section. The two screws at the bottom of the holder are used to clamp the cell to the optical system.

Brinkmann Instruments, Inc., Westbury, N.Y.), temperatures can be maintained with 0.1°C accuracy near 40°C in the presence of 5°C fluctuations in the ambient temperature.

To monitor the state of the lipids we measured the ratio of two distinctive bands in the Raman spectrum of the hydrocarbon chains. The sample was illuminated by a Spectra-Physics model 165 Argon ion laser (Spectra-Physics Inc., Laser Products Div., Mountain View, Calif.) with 300 mW of 5,145 Å radiation, and scattered light was analyzed by a Spex 1301 monochromator (Spex Industries, Inc., Metuchen, N.J.) in conjunction with a computer-assisted light detection system, as described previously (6). The rather wide slit setting of 250 μm was employed to maximize light throughout. The Varian 620/i computer was used to repetitively scan the monochromator and also to control the temperature of the sample.

Although any of several sets of Raman band might be chosen to monitor the lipid structure (3, 6), the C-H stretching offers the strongest scattering in the spectrum, and consequently the highest signal-to-noise ratio for a given collection period. Bands in this region are sensitive to the pretransition at ~35°C as well as the main transition at 41.5°C. As a consequence, the ratio of the assymetric to symmetric stretching bands at 2,880 and 2,850 cm^{-1} have been extensively used by our laboratory and others to characterize the state of fluidity of phospholipid bilayers. The observed intensities for all bands vary in a sample such as this upon phase changes, as does the background. Luminescence generally increases upon both melting and premelting, whereas the overall intensity of the C-H stretching region simultaneously decreases. Fig. 2 shows the effect of raising the temperature on the total scattered light at 2,880 cm^{-1}. The changes in intensity at one frequency are not readily converted to an order parameter, as they derive from several causes which are neither well understood nor relevant to our study. A ratio of band intensities should be insensitive to the two perturbing influences.

To save collection time and make these studies compatible with others being conducted in our laboratory (Yager and Peticolas, manuscript in preparation.), we did not scan the entire C-H stretching region as is commonly done. Instead we slewed the monochromator to three characteristic Δcm^{-1} shifts and counted photons for 50 s at each point. The shifts were chosed from analysis of difference spectra from a previous study of DPPC dispersions (6) to give the maximum possible change in peak ratio at the

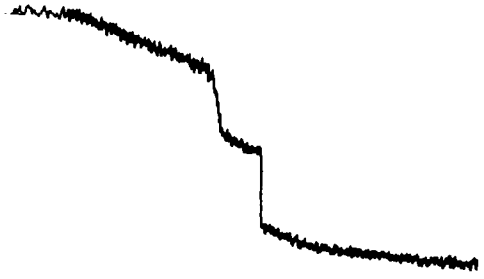

FIGURE 2

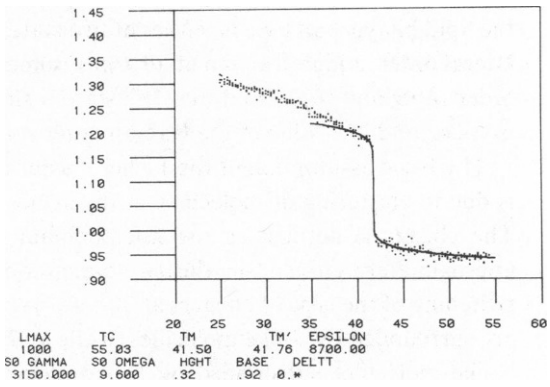

FIGURE 3

FIGURE 2 A photograph of the strip chart recording of the total light received by the monochromator at 2,880 cm^{-1} over a 10 min period as the temperature of the cell was raised from 20°C at the upper left to 47°C ~¼ inch from the right edge. The rate of temperature increase was probably not linear, but the curve does indicate the relative magnitude of changes in light intensity seen through the temperature region. The total decrease was 45% of the light intensity at 20°C.

FIGURE 3 A plot of the observed Raman order ratio vs. temperature (shown as dots), overlayed on the theoretical curve described in the text. The parameters used in the fit are listed at the bottom.

main melting transition. A background point near the region of interest (2,790 cm^{-1}) was used for normalization and to subtract the effects of slow luminescence burn-off. A Raman order ratio (ROR) was generated according to the formula:

$$\mathrm{ROR} = \frac{I_{(2,880)} - I_{(2,790)}}{I_{(2,847.5)} - I_{(2,790)}}.$$

The computer collected 100 intervals of 0.5 s each at the three Δcm^{-1} shifts, performed the above calculation on the 100 sets of three numbers and then averaged the results. Thus each value of the ROR represents 150 s collection time.

For the melting curve shown in Fig. 3, three points were taken at each temperature, with 40-s waiting periods before each to slow collection to ~10 min for every 0.3°C interval, or a heating rate of 1.8°C/h. For the pressure-vs.-order data of Fig. 5 the temperature was held constant at 43.2°C and the pressure increased manually from atmospheric to ~1,500 psig. Data collection was in the same format as the temperature curve, but at least four data were collected at each pressure. The ROR values at each pressure after two runs were pooled, the means and standard deviations calculated, and the results plotted in the figure. All subsequent calculations and plotting were performed in Fortran on a Varian V76 minicomputer (Varian Associates, Palo Alto, Calif.) with Tektronix 4010 and 4662 graphics peripherals (Tektronix Inc., Beaverton, Oreg.).

THERMODYNAMICS AND STATISTICAL MECHANICS OF PRESSURE INDUCED TRANSITIONS IN LIPID BILAYERS

To calculate the change in the Raman order ratio we use an extension of the Fisher cluster theory of phase-transitions which starts from the two dimensional Ising model. The original application of this theory to lipid bilayers was made by Kanehisa and Tsong (9). We extend their work to apply to pressure-induced phase transitions. It is assumed that each molecule in the lipid bilayer can take on either of two states: (*a*) a solid-like "S" state with a high degree of lateral order, a high fraction of all-*trans* isomers, and a consequently high value of the Raman order ratio; and (*b*) a fluid-like "F" state with less lateral interaction, high number of *gauche* isomers, and low value of the Raman order ratio.

The basic assumption of the Fisher cluster theory is that the cooperativity of the transition is due to clustering of molecules in the same state, with each cluster having surface tension. The cluster is defined as the microdomain of nondominant states and is assumed to be approximately circular in the two-dimensional bilayer surface. This definition causes the switching of the type of clusters at $T = T_m$. At $T \leq T_m$ the circular clusters of F-like molecules are surrounded by S-like molecules, while at $T \geq T_m$ the model switches to circular clusters of S-like molecules surrounded by F-like molecules. Thus θ the fraction of S-like or ordered molecules goes from 1 at 0°K to 0 at $T = \infty$°K.

In our extension of the theory to include pressure as a variable, T_m is defined as the melting temperature of the lipid bilayer at a pressure of one atmosphere. Experimentally this is determined as the temperature midway along the abrupt change in order ratio which occurs over a few tenths of a degree at the melting point. Theoretically it is defined as the point at which θ is calculated to be 0.5. The cluster is described by ℓ, the number of molecules in the cluster, and the perimeter length of s molecules on the circular boundary. The assumed circular boundary is reasonable if the melting temperature is sufficiently below the critical

temperature, T_c, and the surface tension of the cluster, γ, is sufficiently large. It is assumed that the mean perimeter length, $\bar{s}$, of an ℓ-sized cluster is given by:

$$\bar{s} = s_0 \ell^{\sigma}, \tag{1}$$

where s_0 is a constant of proportionality; σ is approximately equal to ½ since the linear surface increases approximately as the square-root of the area. In this calculation we take $\sigma = 8/15$ which is the result from an exact solution to the two-dimensional Ising model (9). The constant s_0 is the surface area per molecule and is assumed to be the same for both S and F molecules.

To set up the partition function for an ℓ-sized cluster it is assumed that an F-state molecule has an enthalpy gain of ϵ and an entropy gain of α over a molecule in the S-state. Furthermore, in addition to the surface tension or surface energy, γ, there exists a surface entropy ω. The partion function $q(\ell)$ for an ℓ-sized cluster is then given by

$$q(\ell) = q_0 u^{\ell} v^{\ell^{\sigma}} / \ell^{\tau}, \tag{2}$$

where u and v are defined by the relations:

$$u = \exp(-\epsilon/kT + \alpha/k);\ T < T_m, \tag{3a}$$

$$u = \exp(+\epsilon/kT - \alpha/k);\ T > T_m, \tag{3b}$$

and

$$v = \exp(-s_0\gamma/kT + s_0\omega/k), \tag{4}$$

where k is Boltzman's constant. Eq. 3 gives the criteria for switching cluster types below and above T_m. In Eq. 2 q_0 is a normalization constant and is given by

$$q_0 = \frac{0.5}{\sum_{\ell} \ell^{1-\tau}}, \tag{5}$$

where τ, like σ, is another phenomenological coefficient of the Fisher cluster theory which may be evaluated exactly on the two dimensional Ising lattice as $\tau = 31/15$ (9).

The melting temperature is given as the ratio of the bulk enthalpy to entropy,

$$T_m = \epsilon/\alpha, \tag{6}$$

while the critical temperature is given by the ratio of the surface tension to surface entropy,

$$T_c = \gamma/\omega, \tag{7}$$

In principle, the surface entropy and the proportionality constant, s_0, can be obtained from a knowledge of lattice structure, but in the absence of firm data of the bilayer lattice we have followed Kanehisa and Tsong in using these as adjustable parameters to fit changes in the ROR in the melting region. If n_ℓ is the distribution function for liposomes possessing a cluster of ℓ molecules, then:

$$n_\ell = q_\ell = q_0 u^{\ell} v^{\ell^{\sigma}} / \ell^{\tau}, \tag{8}$$

The order parameter θ is calculated as the fraction of molecules in the S-state and is given by

$$\theta(T) = 1 - \sum_{\ell} \ell n_{\ell};\ T < T_m \tag{9a}$$

and

$$\theta(T) = \sum_{\ell} \ell n_{\ell};\ T > T_m. \tag{9b}$$

The sum goes from one to the number of lipid molecules in a liposome, which we have arbitrarily set equal to an ℓ_{max} of 1,000. From the above equations it is apparent that if $T_m = T_c$ then $\theta = 0.5$ when $u = v = 1$. However, if $T_c \neq T_m$ then $\theta = 0.5$ when u is slightly larger than 1.0 and v is slightly smaller. However the midpoint of the cooperative transition will always occur approximately at $u = 1$.

For computational convenience, and ease in extending the theory to pressures higher than 1 atm it is convenient to express u and v as

$$u = \exp(-\epsilon/RT + \epsilon/RT_m);\ T < T_m, \tag{10a}$$

$$u = \exp(+\epsilon/RT - \epsilon/RT_m);\ T > T_m, \tag{10b}$$

and

$$v = \exp(-s_0\gamma/RT + s_0\gamma/RT_c), \tag{11}$$

where $s_0\gamma$ and ϵ are in units of cal/mol and $R = 1.987$ cal/mol.

As we will show below, using thermodynamically reasonable values for the parameters and combining Eqs. 8–11 gives a sharp cooperative change in θ at $T = T_m$, where $u \simeq v \simeq 1.0$.

Regardless of the area of clusters in the plane of the bilayer, molecules of F-state clusters must occupy a larger volume than those in S-state clusters because of the greater number of gauche rotamers in the hydrocarbon chains above T_m. Measurements of T_m as a function of pressure show a significant linear dependence of T_m on applied hydrostatic pressure, and the ΔV of transition in liter/mol has been measured by several workers (10, 11, 13).

To derive a thermodynamic theory of the pressure-induced phase transition we start with the Clausius equation:

$$\frac{dP}{dT_h} = \frac{\epsilon}{T_h(\Delta V)}\left(\frac{R'}{R}\right), \tag{12}$$

with ϵ in units of cal/mol, ΔV liters/mol, R' is 0.08205 1-atm/mol°K, P is the pressure in atmospheres and T_h is the melting ($\theta = 0.5$) point for $T_h > T_m$. Integration of Eq. 12 gives

$$P = 1 + (R'/R)(\epsilon/\Delta V)\ln(T_h/T_m). \tag{13}$$

If T_h is no more than 40°K above T_m, Eq. 13 may be approximated by

$$P = 1 + (R'/R)(\epsilon/\Delta V)(T_h/T_m - 1). \tag{14}$$

Eq. 14 may be rearranged to give the transition temperature, T_h, as a linear function of the pressure, P, in atmospheres;

$$T_h = T_m[1 + R(\Delta P)(\Delta V)/R'\epsilon], \tag{15}$$

where ΔP is the gauge pressure (psig) or $(P - 1)$ atmospheres.

For the statistical mechanical theory we wish to calculate θ at a temperature $T > T_m$ as a function of the applied hydrostatic pressure, ΔP. Thus Eq. 10b may be generalized to give:

$$u = \exp\left\{\frac{\epsilon}{RT} + \frac{(\Delta P)(\Delta V)}{R'T} - \frac{\epsilon}{RT_m}\right\}, \tag{16}$$

since the enthalpy at pressures higher than 1 atm is given by $\epsilon + \Delta P \Delta V$. As we have mentioned before, the midpoint of the transition is very closely given by $u = 1$. Setting the argument of the exponential function in Eq. 16 equal to zero gives:

$$\frac{\epsilon}{RT_h} + \frac{(\Delta P)(\Delta V)}{R'T_h} - \frac{\epsilon}{RT_m} = 0, \tag{17}$$

which is obviously identical to Eq. 15 which was derived entirely from thermodynamic considerations.

Both Eqs. 10b and 16 are derived assuming that ℓ goes to infinity. For finite ℓ, θ will not equal 0.5 at $T = T_m$. Following Kanehisa and Tsong we define T'_m as the calculated temperature at which $\theta(T'_m) = 0.5$ at 1 atm pressure. If we define P_h as the value of ΔP when $\theta(P_h) = 0.5$, then we may account for the finite patch size in the following way. Below P_h, we are in the region of solid clusters in a fluid matrix:

$$u(P < P_h) = \exp\left(\frac{a\epsilon}{RT} + \frac{\Delta P \Delta V}{R'T} - \frac{\epsilon}{RT_m}\right), \tag{18}$$

where $a = 2T'_m/T_m - 1$. This equation becomes identical to Eq. 16 when $\ell \to \infty$ and $T'_m \to T_m$. It is also identical to Eq. 18 of Kanehisa and Tsong when $\Delta P \to 0$.

For values of $P > P_h$ we are in the region of liquid clusters in a solid matrix; in this case u is given by

$$u(P > P_h) = \exp\left[\frac{a\epsilon}{RT} - \frac{\epsilon}{RT_m} + \frac{(2P_h - \Delta P)\Delta V}{R'T}\right]. \tag{19}$$

Notice that both Eqs. 18 and 19 give the same result when $\Delta P = P_h$. At this pressure $\theta = 0.5$. Using Eqs. 18 and 19, $\theta(P)$ may be calculated from a generalization of Eq. 9: $\theta(P) = \Sigma_\ell \ell n_\ell$ if $\Delta P < P_h$; $T > T_m$ and $\theta(P) = 1 - \Sigma_\ell \ell n_\ell$ if $\Delta P > P_h$; $T > T_m$.

All our pressure experiments were made at $T > T_m$ to observe as complete a change in order as possible from low to high pressure.

RESULTS AND DISCUSSION

The Raman order ratio used in this work is more easily measured with our computerized system than is the Raman order parameter described in earlier work from this laboratory. Since it is based on C-H stretching intensities, changes in the ROR monitor both lateral order

and order along the hydrocarbon chains. This does not, however, invalidate the use of our ratio to monitor the phase transition. Whatever the detailed nature of the patches of liquid and solid lipid in the plane of the bilayer, it is clear from the electron microscopy of bilayers that there is a correlation between temperature and area covered by solid patches (15). Furthermore, the patches are large relative to the size of a single molecule so that aside from a relatively small edge effect most molecules are in either of two states: in an S patch or in an F patch. Since the C-H stretching modes reflect extremely localized conformation not extending past nearest neighbors, the changes in these Raman bands in the temperature range of the phase transition should linearly monitor the number of molecules in the two phases. To compare theory and experiment, the measured Raman data was reduced to the Raman order ratios as described above and plotted as a function of temperature (Fig. 3).

As may be seen in Fig. 3, there is not a specific discontinuity in our ROR at the premelting transition at 35°C, unlike the behavior of the order parameter in the C-H stretching region previously used in this laboratory (9). However, the ROR does show a gradual change in slope at 35°C. The large change in the absolute intensities at 35°C seen in Fig. 2 has been factored out by our selection of a set of Δcm^{-1} shifts which show a maximal change at 41.5°C.

The solid line in Fig. 3 is calculated using Eqs. (9a–b) described previously. Since the calculated value of θ goes from 1 to 0 as T goes from 0° to ∞°K, it was necessary to make certain assumptions in order to overlay the calculated curve on the experimental curve. Based on a slightly different measurement of the ROR (4), the value of the observed ROR could be expected to vary from ~0.9 at high temperatures, >50°C, to nearly 2.0 at −40°C. Because of the presence of the broad pretransition at 35° we could not expect that it would be possible to fit any order parameter to the curve at temperatures below ~38°C if the theory were based on a single transition. The molecular processes leading to ROR changes at temperatures below 38°C are not related to the process of growth of S and L patches we are modeling.

Our assumption that the Raman order ratio, derived as it is from changes in Raman scattering from individual molecules, should change linearly with the proportion of solid and liquid molecules, allowing a direct mapping of the theoretical curve onto the data and greatly simplifying the evaluation of a fit. A less firm assumption is that of the starting and ending points of the transition in the region 35°–55°C mapped by the equation: ROR(Calculated) = [$\theta(T)$ × Height] + Base, where $\theta(T)$ is calculated, Base is the measured ROR at T > 55°C and Height is twice the measured ROR required to match $\theta = 0.5$ to the apparent midpoint of the observed transition. As may be seen from the computer printed output at the bottom of Fig. 3, the Base is near 0.92 and Height 0.32, corresponding to an ROR at 35°C of 1.22. The shape of the calculated curve is fit by adjustment of parameters listed in the computer printout of Fig. 3. In practice, the theoretical parameters were adjusted to produce a curve of the appropriate shape and then Height and Base were chosen to make the calculated curve overlay the experimental points.

Because of the large number of experimental data over the 20°C temperature range, and the fact that a slight change in one of the theoretical parameters changed the shape of the calculated curve dramatically, there was a very limited choice of parameters needed to obtain a really good fit. For example, Fig. 4 shows the fit obtained when T_c (or $s_0\gamma$) varied slightly from the best values shown in Fig. 2.

The values of the theoretical parameters were initially chosen to be identical to those given

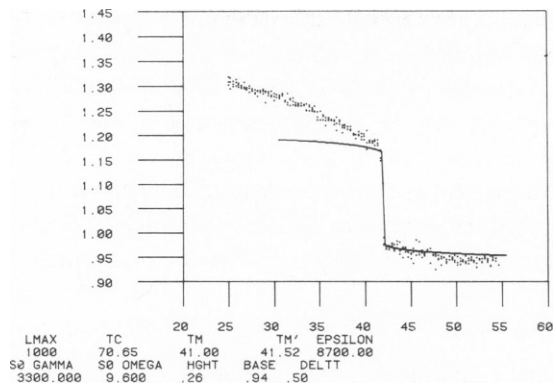

FIGURE 4 A plot similar to that in Fig. 3 in which many of the parameters have been altered slightly to try to obtain the best fit for a maximum patch size of 1,000, but with a *Tc* of 70.65°C. Clearly no manipulations of Height or Base will much improve the fit.

by Kanehisa and Tsong. However, we chose ϵ as 8,700 cal/mol using more recent calorimetric data of Albon et al. (16). We varied two parameters, T_c and ℓ_{max} (the largest patch size). There have been arguments made based on pressure vs. area data in lecithin monolayers that the critical temperature for the multilayer dispersion of DPPC must be ~42°C (17, 18). However we have relaxed this condition during fitting and have found that, within the limits of the theory, a critical temperature between 60° and 80°C gives the most satisfactory fit to the data, particularly if ℓ_{max} is set near 1,000. Calculations with $\ell_{max} > 1{,}000$ were not attempted because of prohibitive computational time and expense.

Once the experimental melting curve was reproduced satisfactorily, it was of interest to see if the experimentally measure pressure-induced order-disorder change could be calculated without further adjustment of the theoretical parameters. With the parameters reported in

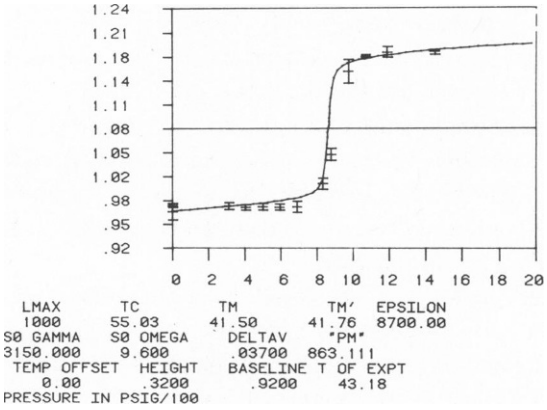

FIGURE 5 An overlay of the theoretical curve generated by the ΔV value of 0.037 liter/mol with the parameters used in Fig. 3 to describe the variation of θ with pressure, with the ROR vs. applied pressure data. The abscissa is in units of 100 psig, while the ordinate is the ROR. The smooth curve is the theoretical curve, while the experimental data are represented as mean values with error bars at 1 SD.

Fig. 3, the only additional parameter needed to calculate the pressure-induced order change is ΔV, the change in molar volume of the multibilayer dispersions between the liquid and solid phases of the lipids, and that has been directly measured by Nagle (10, 11) and indirectly by others and consequently can only be varied within the narrow range of the experimental values.

Using Eq. 20 of the theoretical section, we calculated ROR as a function of P using a ΔV of 0.0370 ml/g, and compared the curve with the experimental results. Both the calculated curve and the experimental results are shown in Fig. 5. This is an experimental confirmation of ΔV.

CONCLUSIONS

The Fisher cluster model as developed for two dimensional lipid bilayers by Kanehisa and Tsong (9) has been extended to include the effect of pressure-induced order-disorder transitions. The agreement between calculated and observed values of the Raman order ratio is within the experimental error of the latter throughout the region of the melting or Chapman transition. However, no theory exists nor was any fit attempted for including the diffuse pretransition at 35°C. Using the observed value of 0.037 for ΔV, the change in molar volume of the pressure-induced changes in ROR were calculated within the experimental error using no new adjustable parameters.

The shape of both pressure-induced and temperature-induced changes in the observed lipid order is quite well accounted for by the theory. The pressure transition shows a sharp cooperative behavior; there is a large change in θ, the fraction of molecules in the S state over a very narrow range in pressure.

A prediction of the cluster model as developed here is that $\theta(P)$ should show a decreasingly cooperative transition at increasingly higher temperatures. This phenomenon should be manifested in two ways. First there may be a smaller change in the cooperative region around the midpoint, P_h', second, the pressure range of the cooperative region may broaden. These phenomena follow from the fact that at $T_m < Tc$, υ is very small. This keeps the perimeter of the cluster a minimum, prevents the formation of more than one cluster per liposome, and is responsible for the observed sharp cooperativity. However, as $T \rightarrow T_c$, $(\gamma - T\omega) \rightarrow 0$ and $\upsilon \rightarrow 1$ so that the cooperativity is lost. Unfortunately we are unable to experimentally measure high enough pressures to test this prediction of the theory.

The temperature or pressure breadth of the transition is due to the model which assumes a finite number of lipid molecules in the liposome. An apparently unrealistic feature of the model is the value of 1,000 for ℓ_{max}, which is too small for the liposomes which we have prepared here. However, phase contrast microscopy does show that these liposomes are closed surfaces some of which are nearly spherical.[1]

Although the cluster model was developed as a mathematical device for statistical mechanical purposes, it has an interesting application to the physical description of order-disorder transition in liposomes. As the spherical or ellipsoidal solid liposome is heated, a circular liquid cluster is formed. As the temperature is raised this cluster grows until it covers an entire hemisphere. As the liquid area becomes > 50% total material, the solid molecules

[1]Yager, P., and W. L. Peticolas. Manuscript submitted for publication.

are constrained to a small circular cluster on the liposome so that the change of the cluster type at T_m occurs automatically because of the topology of the liposome.

Another way of looking at the physical significance of the growing cluster of liquid molecules is to realize that there is an increase in surface area of 40% on going from the solid to the liquid. Thus at the midpoint of the transition, the liquid half of the liposome is larger in area than the solid half. This is exactly what is observed in the microscope, where the reversible growth of the enlarged cluster upon melting is clearly visible. These microscope observations will be discussed in detail in a forthcoming publication.[1]

Finally it should be noted that any breadth in the order-disorder transition due to impurities would affect the analysis. However, it seems clear that completely pure, very small liposomes will have a finite width to their order-disorder transition that can be treated by the model presented here.

We wish to thank Steven Elliott, Siegfried Stolp, and David P. Senkovich of the University of Oregon staff for their assistance with the manufacture of the high pressure apparatus, as well as the James F. Scanlon Company Solvang, Calif., for manufacturing several quartz cells to our specifications.

Support of this work by National Science Foundation grant PCM74-0568 and National Institutes of Health grant GM15547-12 is also gratefully acknowledged.

Received for publication 29 January 1980.

REFERENCES

1. GABER, B. P., P. YAGER, and W. L. PETICOLAS. 1979. Applications of Raman spectroscopy to biomembrane structure. *In* Infrared and Raman Spectroscopy of Biological Molecules. T. M. Theophanides, editor. D. Reidel Publishing Co., Dordrecht, Holland. 241–260.
2. MENDELSOHN, R., and J. MAISANO. 1978. Use of deuterated phospholipids in Raman spectroscopic studies of membrane structure. I. Multilayers of dimyristoyl phosphatidylcholine (and its $-d_{54}$ derivative) with distearoyl phosphatidylcholine. *Biochim. Biophys. Acta.* **506**:192–201.
3. WALLACH, D. F. H., S. P. VERMA, and J. FOOKSON. 1979. Application of laser Raman and infrared spectroscopy to the analysis of membrane structure. *Biochim. Biophys. Acta.* **559**:153–208.
4. YELLIN, N., and I. W. LEVIN. 1977. Hydrocarbon chain disorder in lipid bilayers; temperature dependent Raman spectra of 1,2-diacyl phosphatidylcholine-water gels. *Biochim. Biophys. Acta.* **489**:177–190.
5. GABER, B., and W. L. PETICOLAS. 1977. On the quantitative interpretation of biomembrane structure by Raman spectroscopy. *Biochim. Biophys. Acta.* **465**:260–274.
6. GABER, B., P. YAGER, and W. L. PETICOLAS. 1978. Interpretation of biomembrane structure by Raman differance spectroscopy: nature of the endothermic transitions in phosphatidylcholines. *Biophys. J.* **21**:161–176.
7. GABER, B., P. YAGER, and W. L. PETICOLAS. 1978. Deuterated phospholipids as nonperturbing components for Raman studies of biomembranes. *Biophys. J.* **22**:191–208.
8. GABER, B., P. YAGER, and W. L. PETICOLAS. 1978. Conformational nonequivalence of chains 1 and 2 of dipalmitoyl phosphatidylcholine as observed by Raman spectroscopy. *Biophys. J.* **24**:677–688.
9. KANEHISA, M. I., and T. Y. TSONG. 1978. Cluster model of lipid phase transitions with application to passive permeation of molecules and structure relaxations in lipid bilayers. *J. Am. Chem. Soc.* **100**:424–432.
10. WILKINSON, D. A., and J. F. NAGLE. 1978. A differential dilatometer. *Anal. Biochem.* **84**:263–271.
11. NAGLE, J. F., and D. A. WILKINSON. 1978. Lecithin bilayers: density measurements and molecular interactions. *Biophys. J.* **23**:159–175.
12. TRUDELL, J. R., D. G. PAYAN, J. H. CHIN, and E. N. COHEN. 1974. Pressure-induced elevation of phase

[1] Yager, P., and W. L. Peticolas. Manuscript submitted for publication.

transition temperature in dipalmitoyl phosphatidylcholine bilayers: an electron spin resonance measurement of the enthalpy of phase transition. *Biochim. Biophys. Acta.* **373**:436–443.

13. MACDONALD, A. G. 1978. A dilatometric investigation of the effects of general anaesthetics, alcohols and hydrostatic pressure on the phase transition in smectic mesophases of dipalmitoyl phosphatidylcholine. *Biochim. Biophys. Acta.* **507**:26–37.
14. KAMAYA, H., I. UEDA, P. S. MOORE, and H. EYRING. 1979. Antagonism between high pressure and anesthetics in the thermal phase-transition of dipalmitoyl phosphatidylcholine bilayer. *Biochim. Biophys. Acta.* **550**:131–137.
15. LUNA E. J., and H. M. MCCONNELL. 1977. The intermediate monoclinic phase of phosphatidylcholines. *Biochim. Biophys. Acta.* **466**:381–392.
16. ALBON, N., and J. M. STURTEVANT. 1978. Nature of the gel to liquid crystal transition of synthetic phosphatidylcholines. *Proc. Natl. Acad. Sci. U.S.A.* **75**:2258–2260.
17. PHILLIPS, M. C., and D. CHAPMAN. 1968. Monolayer characteristics of saturated 1,2-diacyl phosphatidylcholines (lecithins) and phosphatidylethanolamines at the air-water interface. *Biochim. Biophys. Acta.* **163**:301–313.
18. HUI, S. W., M. COWDEN, D. PAPAHADJOPOULOS, and F. PARSONS. 1975. Electron diffraction study of hydrated phospholipid single bilayers. Effects on the temperature, hydration, and surface pressure of the "precursor" monolayer. *Biochim. Biophys. Acta.* **382**:265–275.